Size-Selective Fractionation of Nanoparticles at an Application Scale Using CO_2 Gas-Expanded Liquids

Steven R. Saunders, and Christopher B. Roberts*
Department of Chemical Engineering, 212 Ross Hall, Auburn University, AL USA 36849
croberts@eng.auburn.edu, Phone: 1-334-833-4827, Fax: 1-334-844-2063

Size-based fractionation of nanoparticles remains a non-trivial task for the preparation of well-defined nanomaterials for certain applications and fundamental studies. Typical fractionation techniques prove to be inefficient for larger nanoparticle quantities due to the amount of organic solvent required and long processing times. Through the use of the pressure-tunable, physico-chemical properties of CO_2 gas-expanded liquids, a rapid, precise, and environmentally sustainable size-selective fractionation of ligand-stabilized nanoparticles is possible through simple variations in applied CO_2 pressure. This size-selective fractionation technique is based on the controlled reduction of the solvent strength of organic phase nanoparticle dispersions through increases in concentration of an anti-solvent (CO_2) via pressurization. These changes in solvent strength affect the subtle balance between the osmotic repulsive forces (due to the solvation of the stabilizing nanoparticle ligand tails) and the van der Waals forces of attraction between different sized nanoparticles necessary to maintain a stable dispersion. Through modest changes in CO_2 pressure, increasingly smaller nanoparticles can be controllably precipitated from the dispersion, resulting in the separation of particle dispersions ranging from 2nm to 12 nm into ±1nm fractions. An apparatus capable of fractionating large quantities of nanoparticles into distinct fractions has been developed consisting of vertically mounted high pressure vessels connected in series with high pressure needle valves that allow for sequential isolation and separation of the fractionated nanoparticle dispersion. This process at current design scales, operated at room temperature and CO_2 pressures between 0 and 50 bar, can result in a batch or semi-continuous size selective separation of a concentrated nanoparticle dispersion.

INTRODUCTION

Materials with nanoscale dimensions exhibit very unique mechanical, chemical, magnetic, electronic and optical properties which are found neither in at bulk scales nor at the molecular scale [1]. These unique properties are found to be highly size-dependent, and as such, obtaining monodisperse samples of nanoparticles is of the upmost importance for certain applications and fundamental studies. Methods of obtaining monodisperse fractions from polydisperse samples range from size-exclusion and high performance liquid chromatography [2-4], to gel and isoelectric focusing electrophoresis [5, 6], to diafiltration [7]. However, each of these techniques require expensive, specialized equipment and provides a low-throughput. A common technique used to size-selectively fractionate nanoparticles is a liquid solvent-antisolvent technique however this method produces large quantities of organic solvent waste and requires centrifugation [8]. Through the use of gas-expand liquids (GXL's) a similar system can be used without producing the solvent waste or requiring centrifugation.

GXL's are mixtures of an organic solvent and a moderate-pressure gas, which at partial pressures below the vapor pressure of the gas, the gas partitions into the liquid phase allowing for the properties of the medium to be tuned between those of the

organic solvent and those of the gas by simply varying the applied pressure of the gas [9]. In previous studies by our group [10-12], CO_2 was used as an antisolvent in a GXL system to size-selectively precipitate ligand-stabilized metal nanoparticles into narrow sized fractions through simple variations in applied CO_2 pressure. Nanoparticles remain dispersed in a solvent when the solvent-ligand interaction provides a sufficient repulsive force (osmotic repulsive force due to the solvation of the ligand tail by the solvent) to overcome the van der Waals forces of attraction between the nanoparticles. The degree of solvent-ligand interaction is reduced upon the gradual addition of CO_2, a known nonsolvent (or antisolvent) of nonpolar ligands, through pressurization thereby enabling gradual size-dependent precipitation. The magnitude of van der Waals attractive forces between nanoparticles scales with particle size and thus the largest nanoparticles precipitate first upon worsening solvent conditions. Therefore, by precisely adjusting the applied CO_2 pressure, the dispersability of nanoparticles can be controlled to obtained monodisperse particle fractions. It was shown, through the use of a novel Archimedes-type spiral screw, that a polydisperse sample of metal nanoparticles could be fractionated into narrow size-distributions (±1nm) [10]. This apparatus was designed as a proof-of-concept device and was never intended to be scaled-up. In order to produce application-scale quantities (milligram quantities) of monodisperse nanoparticles, a new apparatus needed to be designed that would allow for the investigation of this phenomenon at larger scales.

MATERIALS AND METHODS

Chloroform (99.8% purity), silver nitrate (99.9995%) ($AgNO_3$), and tetraoctylammonium bromide (98%) were obtained from Alfa Aesar. Deionized water (D-H_2O) and toluene (99.8%) were obtained from Fisher. Hydrogen tetrachloroaurate trihydrate (99.9+%) ($HAuCl_4 \cdot 3H_2O$), sodium borohydride (99%), hexane (97+%), and 1-dodecanethiol (98+%) were obtained from Sigma-Aldrich. Ethanol (200 proof) was obtained from Pharmco-Aaper. Carbon Dioxide (SCF/SFE grade) was obtained from Airgas. All chemicals were used as obtained without further purification.

Dodecanethiol-stabilized gold and silver nanoparticles were synthesized by the two-phase arrested precipitation method developed by Brust et al. [13] and later modified by Sigman et al. [14]. This method produces nanoparticles ranging in diameter from 2 to 12 nm with a wide size distribution. Hexane dispersions of metallic nanoparticles were used for all experiments.

A cascaded-vessel apparatus was designed and fabricated to allow for the separation of application-scale quantities of nanoparticle dispersions into monodisperse fractions from an initially polydisperse by through controlling the location of particle precipitation induced via CO_2-pressurization. The primary components of this apparatus are three high-pressure Jerguson gages (R-20) each with an interior volume of approximately 40 mL. Side ports were machined into the Jerguson gages to deliver CO_2 to each vessel independently and to prevent vapor blocks. The fittings for the bottom of the vessels were specially machined with a conical shape to prevent entrainment of liquid. Glass-tube inserts were fabricated to fit into the high-pressure vessel and make a liquid-tight seal with the fitting attached to the bottom of the vessel. The vessels were connected to each other in series with high-pressure needle valves which allows for the complete isolation of one vessel from the others. A high-pressure syringe pump (ISCO 260D) was used to controllably deliver CO_2, however, a simpler system utilizing a CO_2 tank and regulator may be used as all experiments are conducted under the vapor pressure of CO_2. A pressure transducer attached to the top of the cascade is used to

monitor system pressure. Unlike other current nanoparticle size-separation techniques, this apparatus consists of relatively inexpensive and common moderate-pressure equipment.

A typical fractionation was initiated by introducing up to 20 mL of a concentrated nanoparticle-hexane dispersion into the top vessel; with all the isolation valves closed the nanoparticle dispersion remained in the top vessel. The system was then sealed and slowly pressurized to a pressure determined *a priori*. The pressure was carefully controlled using the syringe pump until the system reached equilibrium, which could take as long 90 minutes depending on the pressure range. During this time, the largest fraction of nanoparticles, those which could no longer be stabilized in the solvent mixture at this CO_2 partial pressure, precipitated from solution and adhered to the glass-tube insert via van der Waals interactions. In order to separate the remaining smaller nanoparticles, which were still dispersed in the solvent mixture, the isolation valve separating the top two vessels was slowly opened in order to allow gravity to drain the dispersed nanoparticles away from the nanoparticles that have been precipitated on the inner surfaces of the glass tube contained in the top vessel. This transfer was done slowly and at constant pressure to ensure the precipitated nanoparticles were not sheared off the glass-tube insert nor redispersed due to a change in pressure. After the nanoparticles were transferred to the second vessel, the system was again slowly pressurized to a second pressure, determined *a priori*, during which the largest nanoparticles that were still dispersed precipitated from solution. The smallest, still dispersed nanoparticles were slowly drained into the third vessel while maintaining constant pressure throughout the system. The isolation valves between each vessel were then closed and the system slowly depressurized. The glass-tube inserts were removed from each vessel and washed with hexane to recollect the precipitated fractions. TEM micrographs were acquired on a Zeiss EM 10 Transmission Electron Microscope and sized using ImageJ.

RESULTS

An original sample of 20 mL (approximately 300 mg of metal) of dodecanethiol-stabilized gold nanoparticles dispersed in hexane was used for a single pass fractionation. Previous UV-VIS studies of gold nanoparticle dispersions in CO_2-expanded hexane revealed that precipitation occurs gradually between 40 – 49 bar [11]. Pressure intervals for this fractionation were selected as 0 – 41 bar (Fraction 1) and 41 – 45 bar (Fraction 2). Nanoparticles that could not be precipitated at 45 bar were also collected (Fraction 3). The pressure interval for the first fraction was chosen such that there is a small change in pressure difference between the pressure necessary to induce nanoparticle precipitation and the final pressure of this fraction such that a narrow fraction is obtained. The pressure interval for the second fraction was chosen such that it would provide a similar but narrower size distribution when compared to the original fraction. TEM micrographs and size distributions of the original sample and each fraction can be seen in Figure 1. At least 1000 particles from several locations on each TEM grid were sized such that a statistically relevant sample of the population was investigated. A statistical summary of the size distributions is presented in Table 1.

As can be seen qualitatively in Figure 1 and more quantitatively in Table 1, the same general phenomenon observed using the benchtop-scale apparatus is in fact still obtained at larger scales. The first fraction of particles, those particles collected between 0 – 41 bar, are the largest nanoparticles (average particle diameter of 6.34 nm). The narrow pressure difference between the onset of nanoparticle precipitation and the

end of the pressure interval provided the narrowest distribution (standard deviation of 0.74 nm and a polydispersity index [15] of 1.01) of all three recovered fractions. A 64% improvement in standard deviation in one stage shows that this system is capable of improving the monodispersity of large quantities of nanoparticle dispersions. More than 41% of the particles are within 5% of the average diameter which is an improvement over liquid-based solvent-antisolvent fractionation only capable of reaching 30% [8] The second fraction, those particles collected between 41 – 45 bar, has a similar mean size as the original sample but is narrower in distribution. The original sample had an average diameter of 6.14 nm where the second fraction has an average diameter of 5.70 nm. This can be improved by simply adjusting the pressure stages.

Sample	Average Diameter (nm)	Standard Deviation (nm)	Polydispersity Index
Original	6.14	1.99	1.11
Fraction 1 (0 – 41 Bar)	6.31	0.74	1.01
Fraction 2 (41 – 45 bar)	5.70	1.36	1.04
Fraction 3 (45+ bar)	4.28	1.56	1.05

Table 1: Statistical summary of a single pass fractionation.

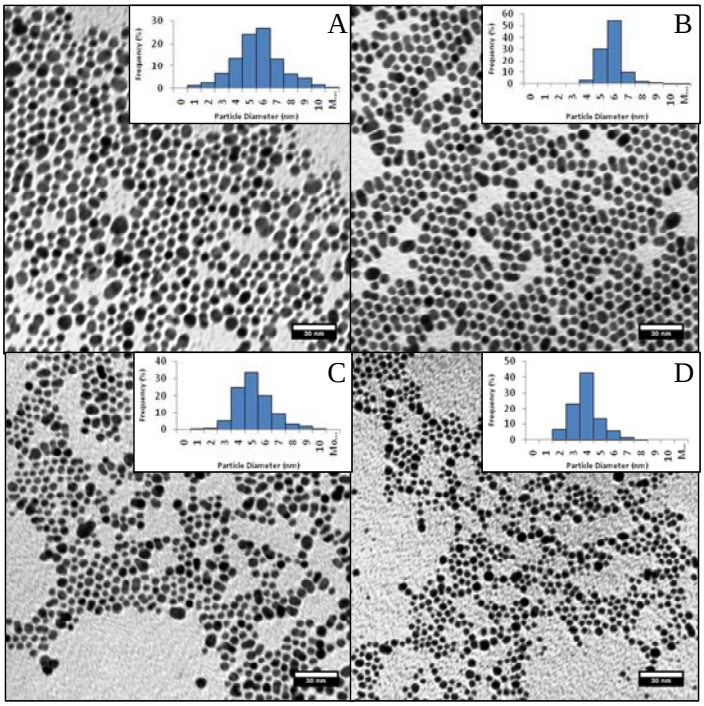

Figure 1 : TEM micrographs of a single pass fractionation. (A) original sample, (B) particles precipitated between 0 – 41 bar, (C) particles precipitated between 41 – 45 bar, and (D) particles collected that were not precipitated at 45 bar. The size distribution of each fraction is inset. Scale bars are 30 nm.

In order to investigate the fractionation effectiveness of the technique, recursive fractionations were performed. Dodecanethiol stabilized silver nanoparticles dispersed in hexane were fractionated at pressure intervals of 0 – 43 bar and 43 – 45 bar. The

nanoparticles that could not be precipitated at 45 bar were also collected. These pressure intervals were chosen such that the second fraction should be the narrowest of the three collected fractions with an average size similar to that of the original sample. The nanoparticles collected at 43 – 45 bar were reintroduced into the top vessel of the apparatus and re-fractionated at the same pressure intervals to see if the distribution would change as a result of the recursive fractionation. A total of three recursive fractionations were performed at the same pressure intervals, each time collecting and analyzing the fraction from the second vessel (nanoparticles precipitated between 43 – 45 bar). TEM micrographs and size distributions of the original sample as well as of the second fractions (43 – 45 bar) from each pass can be seen in Table 2. At least 1000 particles from several locations on each TEM grid were sized such that a statistically relevant sample of the population was investigated. A statistical summary of the size distributions is presented in Table 2.

Sample	Average Diameter (nm)	Standard Deviation (nm)	Relative Standard Deviation	Polydispersity Index
Original	4.38	1.63	37.2	1.14
One Pass	4.14	1.04	25.2	1.06
Two Passes	4.04	0.93	23.1	1.05
Three Passes	4.02	0.74	18.4	1.03

Table 2: Statistical summary of recursive fractionations.

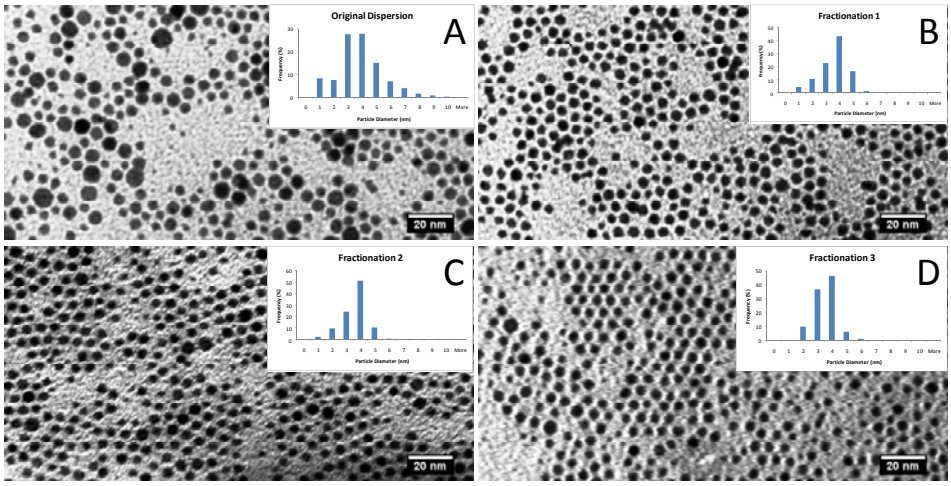

Figure 2: TEM micrographs of recursive fractionations. (A) Original sample, (B) One pass, (C) Two passes, and (D) Three passes. Scale bars are 20 nm.

Each recursive fractionation produced incrementally more narrow fractions. The standard deviation of each sample decreased with each fractionation, improving by 36% after one pass, 43% after two passes, and finally, 55% after three passes. The fractions become monodisperse enough to begin to locally self-assemble into close packed hexagonal-arrays.

CONCLUSION

Utilizing the tunable solvent properties of gas-expanded liquids, application-scale quantities of nanoparticles can be size-selectively fractionated quickly and easily, without the use of expensive equipment nor producing large quantities of waste solvent.

Thiol-stabilized nanoparticles can be precipitated by finely tuning the balance between the van der Waals forces of attraction and the osmotic repulsive forces by simply changing an applied partial pressure of CO_2 above the hexane-nanoparticle dispersion. This technique enables the fractionation of large quantities of polydisperse nanoparticles into very narrow (< ±1 nm), monodisperse fractions with targeted mean diameters (± 0.5 nm)

REFERENCES

[1] ADAIR, J. H., LI T., KIDO T., HAVEY K., MOON J., MECHOLSKY J., MORRONE A., TALHAM D. R., LUDWIG M. H. WANG L., Materials Science & Engineering R-Reports, Vol. 23, **1998**, p. 139

[2] FISCHER, C. H., WELLER H., KATSIKAS L. HENGLEIN A., Langmuir, Vol. 5, **1989**, p. 429

[3] WILCOXON, J. P., MARTIN J. E., PARSAPOUR F., WIEDENMAN B. KELLEY D. F., The Journal of Chemical Physics, Vol. 108, **1998**, p. 9137

[4] JIMENEZ, V. L., LEOPOLD M. C., MAZZITELLI C., JORGENSON J. W. MURRAY R. W., Analytical Chemistry, Vol. 75, **2003**, p. 199

[5] HANAUER, M., PIERRAT S., ZINS I., LOTZ A. SONNICHSEN C., Nano Letters, Vol. 7, **2007**, p. 2881

[6] ARNAUD, I., ABID J. P., ROUSSEL C. GIRAULT H. H., Chemical Communications, Vol. **2005**, p. 787

[7] SWEENEY, S. F., WOEHRLE G. H. HUTCHISON J. E., Journal of the American Chemical Society, Vol. 128, **2006**, p. 3190

[8] MURRAY, C. B., KAGAN C. R. BAWENDI M. G., Annual Review of Materials Science, Vol. 30, **2000**, p. 545

[9] JESSOP, P. G. SUBRAMANIAM B., Chemical Reviews, Vol. 107, **2007**, p. 2666

[10] MCLEOD, M. C., ANAND M., KITCHENS C. L. ROBERTS C. B., Nano Letters, Vol. 5, **2005**, p. 461

[11] ANAND, M., MCLEOD M. C., BELL P. W. ROBERTS C. B., Journal of Physical Chemistry B, Vol. 109, **2005**, p. 22852

[12] ANAND, M., YOU S. S., HURST K. M., SAUNDERS S. R., KITCHENS C. L., ASHURST W. R. ROBERTS C. B., Industrial & Engineering Chemistry Research, Vol. 47, **2008**, p. 553

[13] BRUST, M., WALKER M., BETHELL D., SCHIFFRIN D. J. WHYMAN R., Journal of the Chemical Society, Chemical Communications, Vol. **1994**, p. 801

[14] SIGMAN, M. B., SAUNDERS A. E. KORGEL B. A., Langmuir, Vol. 20, **2004**, p. 978

[15] Polydispersity index is defined as the ratio of the diameter-weighted average diameter $\left(\sum D_i^2 / \sum D_i\right)$ to the number average diameter $\left(\sum D_i / n\right)$ where D_i is the diameter of a given nanoparticle and n is the total number of nanoparticles. A population that is monodisperse (standard deviation of 0 nm) has a polydispersity index of 1. The larger the value of the polydispersity index, the more polydisperse the population is.